Core Excitation Spectroscopy of Phenyl- and Methyl-Substituted Silanol, Disiloxane, and Disilane Compounds: Evidence for π-Delocalization across the Si−C_{phenyl} Bond

Stephen G. Urquhart,[†] Cássia C. Turci,[†,‡] Tolek Tyliszczak,[†] Michael A. Brook,[†] and Adam P. Hitchcock*,[†]

Department of Chemistry, McMaster University, Hamilton, Ontario, Canada L8S 4M1, and Instituto de Química, Universidade Federal do Rio de Janeiro, Rio de Janeiro, Brazil 21910-900

Received December 6, 1996[⊗]

The Si 1s and 2p solid state photoabsorption (total electron yield) spectra of triphenylsilanol, hexaphenyldisiloxane, and hexaphenyldisilane and the Si 1s spectra (total ion yield) of gaseous trimethylsilanol, hexamethyldisiloxane, hexamethyldisilane, and trimethylmethoxysilane have been recorded using synchrotron radiation. These spectra are compared to inner shell electron energy loss spectra of gaseous triphenylsilanol, hexaphenyldisilane, trimethylmethoxysilane, hexamethyldisiloxane, and hexamethyldisilane in the Si 2p and C 1s regions, measured under scattering conditions where electric dipole transitions dominate (2.5 keV residual energy, $\theta \leq 2°$). Comparison of the Si 1s and Si 2p spectra of the Ph_3Si-X and Me_3Si-X species shows there are low-lying transitions at Si which occur exclusively in the Ph_3Si-X species. These transitions are attributed to (Si $1s^{-1}$,π^*_{Si-Ph}) and (Si $2p^{-1}$,π^*_{Si-Ph}) states in which the core excited electron is delocalized across the Si−C(phenyl) bond into the π^* levels of the phenyl ring. Extended Hückel and *ab initio* molecular orbital calculations of the core excitation spectra support this interpretation. Transitions characteristic of Si−Si and Si−O bonds are also identified.

1. Introduction

During the past five decades, the unique properties and industrial potential of organosilicon compounds, including silicone polymers, elastomers, and resins, have been recognized and these materials have become major industrial products.[1−3] Silicones have desirable thermal and oxidative stability, flexibility, inertness and radiation resistance. Polymethylphenylsilicones and polydiphenylsilicones, in particular, are more stable to oxidation, high temperature decomposition, and radiation damage than methylsilicones,[4] with the rupture of methyl groups occurring preferentially over phenyl groups at high temperatures.[5] Aromatic stabilization by the phenyl group has been postulated as the origin of this increased stability.[4,6] This work continues our study of the sensitivity of core excitation spectroscopy to chemical properties and bonding in organosilanes. We examine the effects of π^* and σ^* delocalization associated with Si−phenyl (Si−Ph), Si−Si, and Si−O bonding, focusing in particular on the nature of π^* delocalization across the Si−phenyl bond.

A study of the electronic spectroscopy of organosilanes must be considered in the context of organosilane bonding models. In Si−Ph and Si−O containing species, hyperconjugation and (d−p)π bonding[7] models have been invoked to explain spectral and physical characteristics. In the hyperconjugation model, phenyl 2pπ electrons (or the oxygen lone pair electrons in the case of Si−O bonding) are delocalized into vacant σ^* levels on silicon. In the (d−p)π bonding model, the 2pπ electrons are delocalized into unoccupied Si 3d orbitals[7] although recent studies are critical of the (d−p)π bonding model for silicon.[8] While the large Si−O−Si bond angles and bond flexibility in oxo-bridged organosilanes have been rationalized in terms of hyperconjugation and (d−p)π bonding, it has also been argued that the dominant ionic character of the Si−O bond, and the resulting weak localization of electron pair domains on oxygen, is the origin of this effect.[9,10] Through comparison of the core excitation spectra, we have explored the covalent versus ionic character of Si−O bonding.

Core excitation spectroscopy is a site-specific spectroscopic technique offering detailed information concerning the unoccupied electronic structure of molecules or extended systems. Core excitation can be studied by

[†] McMaster University.
[‡] Universidad de Federal do Rio de Janeiro.
[⊗] Abstract published in *Advance ACS Abstracts,* April 15, 1997.

(1) Greenwood, N. N; Earnshaw, A. *Chemistry of the Elements*; Pergamon Press: Cambridge, 1984.
(2) *The Chemistry of Organic Silicon Compounds*; Patai S., Rappoport, Z., Eds.; Wiley: New York, 1989.
(3) Walsh, R. Thermochemistry. In *The Chemistry of Organic Silicon Compounds*; Patai, S., Rappoport, Z., Eds.; Wiley: New York, 1989.
(4) Noll, W. *Chemistry and Technology of Silicones*; Academic Press: New York, 1968. Kennan, J. J. In *Siloxane Polymers*; Clarson, S. J., Semlyen, J. A., Eds.; PTR Prentice Hall: Englewood Cliffs, NJ, 1993; Chapter 2, pp 72−134.
(5) Murphy, C. M.; Saunders, C. E.; Smith, D. C. *Ind. Eng. Chem.* **1950**, *42*, 2462.
(6) Miller, A. A. *I&EC Prod. Res. Dev.* **1964**, *3*, 1964.
(7) Kwart, H.; King, K. G. *d-Orbitals in the Chemistry of Silicon, Phosphorus and Sulfur*; Springer: Berlin, 1977. Reed, A. E.; von Ragué Schleyer, P. *J. Am. Chem. Soc.* **1990**, *112*, 1434.
(8) Shambayati, S.; Blake, J. F.; Wierschke, S. G.; Jorgensen, W. L.; Schreiber, S. L. *J. Am. Chem. Soc.* **1990**, *112*, 697.
(9) Bader, R. F. W. *Atoms in Molecules: A Quantum Theory*; Oxford: New York, 1990.
(10) Gillespie, R. J.; Johnson, S. A. *Inorg. Chem.*, submitted for publication.

S0276-7333(96)01028-X CCC: $14.00

X-ray photoabsorption[11] or electron energy loss spectroscopy.[12] A bibliography and data base of gas phase core excitation studies has been published recently.[13] Several recent studies[14−18] have investigated the relationship between Si and ligand near edge spectral features and the local structure around Si in organosilicon compounds. In some cases, these studies have combined synchrotron radiation and electron energy loss results of the same species in the solid and/or gas phase (where volatility permits) with quantum chemical calculations.[17,18] The combination of multiple edge spectra with calculations makes core excitation spectroscopy a powerful probe of the molecular electronic structure.

In this work, we have used core excitation spectroscopy to study delocalization across the Si−phenyl bond and oxygen lone pair delocalization in Me_3SiO-X and Ph_3SiO-X species. We have also extended our earlier studies of low-lying σ^*_{Si-Si} features in disilanes (Si−Si).[16,17] In particular, we present inner shell electron energy loss spectra (ISEELS) in the Si 2p and C 1s region of *gas* phase triphenylsilanol (Ph_3SiOH), hexaphenyldisilane ($Ph_3SiSiPh_3$), hexamethyldisiloxane ($Me_3SiOSiMe_3$), hexamethyldisilane ($Me_3SiSiMe_3$), and trimethylmethoxysilane (Me_3SiOMe), recorded under experimental conditions dominated by electric dipole transitions. We also present total electron yield (TEY) spectra in the Si 1s and Si 2p region of *solid* phase triphenylsilanol (Ph_3SiOH), hexaphenyldisiloxane ($Ph_3SiOSiPh_3$), and hexaphenyldisilane ($Ph_3SiSiPh_3$), as well as total ion yield (TIY) spectra in the Si 1s region of *gas* phase trimethylsilanol (Me_3SiOH), hexamethyldisiloxane ($Me_3SiOSiMe_3$), trimethylmethoxysilane (Me_3SiOMe), and hexamethyldisilane ($Me_3SiSiMe_3$). Comparison of the spectra for the methyl- and phenyl-series has identified features related to Si−C, Si−Si, or Si−O bonds in a given compound and identified delocalization of phenyl π^* density across the Si−C(Ph) bond in Ph_3Si-X molecules.

2. Experimental Section

2.1. Samples. Triphenylsilanol (Ph_3SiOH), trimethylmethoxysilane (Me_3SiOMe), and hexamethyldisiloxane ($Me_3SiOSiMe_3$) (purchased from Aldrich, ≥98% purity), hexaphenyldisilane ($Ph_3SiSiPh_3$), hexamethyldisilane ($Me_3SiSiMe_3$), and hexaphenyldisiloxane ($Ph_3SiOSiPh_3$) (purchased from Hüls America, ≥98% purity) were used without further purification. Trimethylsilanol (Me_3SiOH) was prepared according to a literature method.[19] Spectra of trimethylsilanol were acquired within 6 h of synthesis, before any significant dimerization had occurred. All compounds were handled in a glovebag flushed with dry nitrogen in order to minimize hydrolysis. Liquid samples were loaded in dried glass vacuum flasks and were subjected to several freeze−pump−thaw cycles to remove dissolved gases. For Si 1s and 2p photoabsorption, the solid samples were mounted by pressing the sample powder into a copper surface that was previously pitted with strong nitric acid.

2.2. Electron Energy Loss Spectroscopy. The gas phase ISEELS spectrometer employed in these experiments has been described in detail previously.[12] The spectrometer is operated under conditions of small momentum transfer (2.5 keV impact energy, small (<2°) scattering angle) where the electronic excitations are dominated by electric-dipole-allowed transitions. The overall energy resolution, which is typically 0.6−0.7 eV full width at half maximum (fwhm), is determined by the convolution of the energy width of the unmonochromatized incident electron beam (∼0.4 eV) and the analyzer acceptance (∼0.4 eV).

The volatile samples (Me_3SiOH, $Me_3SiOSiMe_3$, Me_3SiOMe, $Me_3SiSiMe_3$) were introduced into the collision cell through a leak valve. The involatile Ph_3SiOH and $Ph_3SiSiPh_3$ samples were placed directly inside the spectrometer in a heatable glass tube attached to the collision cell. Spectra of Ph_3SiOH were obtained at a number of different heating conditions in order to confirm reproducibility and to check if sample heating might lead to thermal decomposition. The same procedure was not possible for $Ph_3SiSiPh_3$ due to the difficulty in maintaining an adequate sample pressure in the gas cell. For this reason, the ISEEL spectra of this compound are of lower statistical quality. The stability on heating was also checked for both compounds by electron impact mass spectrometry. The mass spectrum of Ph_3SiOH did not change until the sample was heated above 200 °C while that of $Ph_3SiSiPh_3$ was only observed to change when the temperature was above 550 °C.

The energy loss scale was established by simultaneously recording the spectrum of the sample with that of two reference compounds: CO_2, using the C 1s → π* (290.74(4) eV) transition,[20,21] and SF_6, using the S $2p_{1/2} \rightarrow t_{2g}$ (184.54(5) eV) transition.[20] The signal associated with a particular core edge was isolated from the underlying valence shell and core ionization continua by subtracting a smooth curve determined from a curve fit of the function $a(E - b)^c$ to the pre-edge experimental signal. The C 1s background-subtracted spectra were converted to absolute oscillator strength scales by using a method described and tested previously.[13] The Si 2p background-subtracted spectra were converted to absolute oscillator strengths by normalizing to the absolute Si 2p oscillator strength of SiH_4 in the region of 145−151 eV.[22] This featureless, atomic-like region is higher in energy than the prominent Si 2p → εd transitions in the continuum and before the onset of the Si 2s edge.

2.3. Synchrotron Radiation Studies. 2.3.1. Si 1s Spectra. The Si 1s spectra of the solid Ph_3SiOH, $Ph_3SiOSiPh_3$, and $Ph_3SiSiPh_3$ samples were measured by total electron yield (TEY) detection, and the gas Me_3SiOH, $Me_3SiOSiMe_3$, Me_3SiOMe, and $Me_3SiSiMe_3$ samples were measured by total ion yield (TIY) detection, using the double-crystal monochromator[23] of the Canadian Synchrotron Radiation Facility (CSRF) located at the Synchrotron Radiation Center (SRC) in Wisconsin. This monochromator is equipped with InSb crystals and has an energy resolution of 0.8 eV at 1840 eV. The absolute energy scale was set by prior recording of the total electron yield spectrum of crystalline silicon (c-Si).

(11) Stöhr, J. *NEXAFS Spectroscopy*; Springer-Verlag: Berlin, 1992.
(12) Hitchcock, A. P. *Phys. Scr.* **1990**, *T31*, 159.
(13) Hitchcock, A. P.; Mancini, D. C. *J. Electron Spectrosc. Relat. Phenom.* **1994**, *67*, 1.
(14) Hitchcock, A. P.; Tyliszczak, T.; Aebi, P.; Xiong, J. Z.; Sham, T. K.; Baines, K. M.; Mueller, K. A.; Feng, X. H.; Chen, J. M.; Yang, B. X.; Lu, Z. H.; Baribeau, J. M.; Jackman, T. E. *Surface Sci.* **1993**, *291*, 350.
(15) Sutherland, D. G. J.; Kasrai, M.; Bancroft, G. M.; Liu, Z. F.; Tan, K. H. *Phys. Rev. B.* **1993**, *48*, 15089.
(16) Urquhart, S. G.; Xiong, J. Z.; Wen, A. T.; Sham, T. K.; Baines, K. M.; de Souza, G. G. B.; Hitchcock, A. P. *Chem. Phys.* **1994**, *189*, 757.
(17) Xiong, J. Z.; Jiang, D. T.; Liu, Z. F.; Baines, K. M.; Sham, T. K.; Urquhart, S. G.; Wen, A. T.; Tyliszczak, T.; Hitchcock, A. P. *Chem. Phys.* **1996**, *203*, 81.
(18) Urquhart, S. G.; Hitchcock, A. P.; Denk, M. *J. Am. Chem. Soc.*, submitted for publication.
(19) Sommer, L. H.; Pietrusza, E. W.; Whitmore, F. C. *J. Am. Chem. Soc.* **1946**, *68*, 2282.
(20) Sodhi, R. N. S.; Brion, C. E. *J. Electron Spectrosc. Relat. Phenom.* **1984**, *34*, 363.
(21) Brion, C. E.; Daviel, S.; Sodhi, R.; Hitchcock, A. P. *AIP Conf. Proc.* **1982**, *94*, 429.
(22) Cooper, G.; Ibuki, T.; Brion, C. E. *Chem. Phys.* **1990**, *140*, 147. Cooper, G.; Burton, G. R.; Chan, W. F.; Brion, C. E. *Chem. Phys.* **1995**, *196*, 293.
(23) Yang, B. X.; Middleton, F. H.; Olsson, B. G.; Bancroft, G. M.; Chen, J. M.; Sham, T. K.; Tan, K.; Wallace, D. J. *Nucl. Instrum. Methods* **1992**, *A316*, 422.; *Ibid. Rev. Sci. Instrum.* **1992**, *63*, 1355.

The inflection point of the absorption edge of c-Si (determined by the peak in the first derivative) was set to 1839.2 eV.[14,24]

The TEY spectra of the solid samples were obtained by measuring the sample current associated with all electrons emitted from the sample after the absorption of an X-ray photon (elastic, Auger, photoelectrons, and inelastically scattered electrons). The TIY spectra of gases were obtained by measuring the photoion current, using a 10 cm long parallel plate ionization chamber. The sample pressure was measured with a baratron gauge, and this signal was used to correct for (minor) pressure variations during acquisition. In addition, the gas phase spectra were scaled by $1/E$ to correct for the intrinsic bolometric effect of ionization current detection.[25] The incident photon flux (I_0) at the Si 1s edge was monitored using an inline gas ionization chamber equipped with thin Be windows. The I_0 signal was used to normalize the TEY and TIY spectra. Normalized and calibrated TEY and TIY spectra were background-subtracted to isolate the Si 1s core edge signal, and the results were converted to absolute oscillator strength intensity scale by normalization to the atomic value of 1.6×10^{-3} eV^{-1} at 1860 eV.[26]

2.3.2. Si 2p Spectra. The Si 2p spectra of the solid Ph_3SiOH, $Ph_3SiOSiPh_3$, and $Ph_3SiSiPh_3$ samples were measured by TEY detection using the Mark IV Grasshopper monochromator[27] of the Canadian Synchrotron Radiation Facility at SRC. For these experiments, the monochromator was run with 30 μm slits for an energy resolution of ~0.15 eV fwhm. The energy scale of this monochromator was calibrated by setting the energy of the first peak of the derivative of the Si 2p spectrum of c-Si to 99.804 eV. This value for the first inflection point in the Si 2p spectrum of c-Si is based on a careful calibration of its energy with respect to the Si $2p_{3/2} \rightarrow a_1^*$ transition of SiF_4.[28] The absolute energy scales are estimated to be accurate to within 0.1 eV in the region between 100 and 200 eV. For most of the pre-edge absorption features, the monochromator resolution is the limiting factor in determining the positions of the sharp discrete resonances. In the continuum regions, resonances are much broader and the estimated error in their position is 0.5 eV. The incident photon flux (I_0) was measured simultaneously using the photocurrent from a clean Ni mesh placed in the photon beam before the sample. The I_0 signal is used to normalize the TEY spectra. The spectra were background-subtracted and normalized to the Si 2p oscillator strength spectrum of SiH_4, as described in section 2.2.

2.4. Calculations. The core excitation spectra of phenylsilanes have been interpreted with the aid of extended Hückel molecular orbital (EHMO) as well as *ab initio* calculations of simple model molecules. EHMO calculations of the Si 1s spectra of Ph_3SiH and $PhSiH_3$ were carried out with the CACAO program[29] using the default Hückel parameters[30] calculated without d orbitals. Predictions of the Si 1s core excitation spectra were generated by EHMO calculations using the equivalent ionic core virtual orbital model (EICVOM),[31] with procedures described previously.[32,33] In this model, core hole relaxation is approximated by replacing the core excited atom by its "$Z + 1$" equivalent (e.g., silicon by phosphorus) and setting the molecular charge to +1.

Ab initio calculations of the Si 1s core excitation spectrum of $PhSiH_3$ and $PhSiMe_3$ were carried out with the program GSCF3.[34] This program treats core hole relaxation by explicit inclusion of the core hole.[35] The basis set used for this calculation is the extended basis set taken from (533/53) and (63/5) contracted Gaussian-type functions for Si and C and (5) for H of Huzinaga et al.,[36] where the contraction scheme was (311111111/311111/1*) for the core excited silicon, (621/41) for the carbon atoms, and (41) for H. The core excited states were obtained with the improved virtual orbital (IVO) method.[37] The relaxed Hartree−Fock (HF) potential is essential in accurately considering large electronic reorganization upon inner shell hole creation; therefore, the IVO method based on the relaxed HF potential is superior to the method using the ground state orbitals. This method has been shown to be quite accurate in predicting term values and intensities of core excitations.[38−40]

The program SPARTAN[41] was used to provide the geometry-optimized structures of Ph_3SiH, Ph_3SiH, and $PhSiMe_3$ at the *ab initio* HF/3-21G* level. These geometries were used for both the EHMO and *ab initio* core excitation calculations. Gaussian line widths used in generating the predicted spectra from both the EHMO and *ab initio* results were 4 eV fwhm for orbitals of eigenvalue (ϵ) above 3 eV 2 eV for $0 < \epsilon < 3$, and 0.6 eV for $-15 < \epsilon < 0$ eV. The energy scales of the EHMO-predicted spectra were set by matching the first calculated transition to the first experimental transition of Ph_3SiOH. Relative to aligning the zero of the Hückel eigenvalue scale to the *estimated* ionization potential (IP), alignment at the first experimental transition requires energy shifts of +3.0 eV for $PhSiH_3$ and Ph_3SiH. The energy scales of the *ab initio* calculated spectra were set by setting the zero of the term value scale to the ionization potentials calculated by GSCF3 (1843.11 eV for $PhSiH_3$; 1842.41 eV for $PhSiMe_3$).

3. Results and Discussion

3.1. Si 1s Spectra. Figure 1 presents the Si 1s oscillator strength spectra for three Ph_3Si-X molecules (X = $SiPh_3$, $OSiPh_3$, and OH) and four Me_3Si-X species (X = $SiMe_3$, $OSiMe_3$, OMe, and OH). Energies, term values, and tentative assignments for the Si 1s spectra are presented in Table 1. The energy scale for presenting the disilane spectra ($Me_3SiSiMe_3$ and $Ph_3SiSiPh_3$; top scale) is shifted by 1.3 eV relative to that for the triphenyl and trimethyl Si−O species ($Ph_3SiOSiPh_3$, Ph_3SiOH, $Me_3SiOSiMe_3$, Me_3SiOMe, and Me_3SiOH; bottom scale). This shift is introduced to account for the ~1 eV difference in the ionization potentials of the disilane (Si−Si)- and the Si−O-bonded species, since states of a similar final orbital character usually have similar core excitation term values (TV = IP − E).

The most dramatic difference in the Si 1s spectra is the dominant low-lying peak around 1842 eV in the spectrum of each Ph_3Si-X species (X = OH, $OSiPh_3$, $SiPh_3$). We attribute this feature to Si 1s $\rightarrow \pi^*_{Si-Ph}$ excitations, where π^*_{Si-Ph} refers to an orbital involving

(24) McGrath, R.; McGovern, I. T.; Warburton, D. R.; Purdie, D.; Muryn, C. A.; Prakash, N. S.; Wincott, P. L.; Thornton, G.; Law, D. S. L.; Norman, D. *Phys. Rev. B* **1992**, *45*, 9327.
(25) Hitchcock, A. P.; Tronc, M. *Chem. Phys.* **1988**, *121*, 265.
(26) Henke, B. L.; Lee, P.; Tanaka, T. L.; Shimabukuro, R. L.; Fujikawa, B. K. *At. Data Nucl. Data Tables* **1982**, *27*, 1.
(27) Tan, K. H.; Bancroft, G. M.; Coatsworth, L. L.; Yates, B. W. *Can. J. Phys.* **1982**, *60*, 131.
(28) Bozek, J. D.; Bancroft, G. M.; Tan, K. H. *Chem. Phys.* **1990**, *145*, 131.
(29) Meali, C.; Proserpio, D. M. *J. Chem. Educ.* **1990**, *67*, 399.
(30) Howell, J.; Rossi, A.; Wallace, D.; Haraki, K.; Hoffmann, R. *FORTICON8 Program QCMP011 from Quantum Chemical Program Exchange;* Indiana University: Bloomington, IN, 1982.
(31) Schwarz, W. H. E. *Chem. Phys.* **1975**, *11*, 217.
(32) Francis, J. T.; Hitchcock, A. P. *J. Phys. Chem.* **1992**, *96*, 6598.
(33) Urquhart, S. G.; Hitchcock, A. P.; Priester, R. D.; Rightor, E. G. *J. Polym. Sci., Part B: Polym. Phys.* **1995**, *33*, 1603.
(34) Kosugi, N. *Theor. Chim. Acta* **1987**, *72*, 150.
(35) Kosugi, N.; Kuroda, H. *Chem. Phys. Lett.* **1980,** *74*, 500.
(36) Huzinaga, S.; Andzelm, J.; Klobukowski, M.; Radzio-Andzelm, E.; Sasaki, Y.; Tatewaki, H. *Gaussian Basis Sets for Molecular Calculations*; Elsevier: Amsterdam, 1984.
(37) Hunt, W. J.; Goddard, W. A., III *Chem. Phys. Lett.* **1969**, *3*, 414.
(38) Kosugi, N.; Shigemasa, E.; Yagishita, A. *Chem. Phys. Lett.* **1992**, *190*, 481.
(39) Kosugi, N.; Adachi, J.; Shigemasa, E.; Yagishita, A. *J. Chem. Phys.* **1992**, *97*, 8842.
(40) Iwata, S.; Kosugi, N.; Nomura, O. *Jpn. J. Appl. Phys.* **1978**, *17-S2*, 109.
(41) *Spartan*, version 4.0; Wavefunction Inc.: Irvine, CA, 1994.

Table 1. Energies, Term Values, and Proposed Assignments for Features in the Si 1s Photoabsorption Spectra of (A) Triphenylsilanol, Hexaphenyldisiloxane, and Hexaphenyldisilane and (B) Trimethylsilanol, Hexamethydisiloxane, Trimethylmethoxylsilane, and Hexamethyldisilane

A. Ph_3Si-X

Ph_3-SiOH[a]		$Ph_3Si-O-SiPh_3$[a]		$Ph_3Si-SiPh_3$[a]		
E (eV)	*T*	*E* (eV)	*T*	*E* (eV)	*T*	assignment
1841.8	5.1	1841.9	5.0	1840.8	4.9	$1\pi^*_{Si-Ph}$
				1842.7	3.0	σ^*_{Si-Si}
				1844.1	1.6	σ^*_{Si-C}, $2\pi^*_{Si-Ph}$
1844.8	2.1	1844.7	2.2			σ^*_{Si-C}, σ^*_{Si-O}, $2\pi^*_{Si-Ph}$
1846.9[b]		1846.9[b]		1845.7[b]		IP
		1849.4	−2.5			$2e^-$
1852.9	−6.0	1852.7	−5.8	1850.1	−4.4	$1\sigma^*_{C=C}$
1863	−16	1862	−15	1862	−16	$2\sigma^*_{C=C}$, EXAFS

B. Me_3Si-X

Me_3-SiOH[a]		$Me_3Si-O-SiMe_3$[a]		$Me_3Si-OMe$[a]		$Me_3Si-SiMe_3$[a]		
E (eV)	*T*	*E* (eV)	*T*	*E* (eV)	*T*	*E* (eV)	*T*	assignment
						1841.5	4.2	σ^*_{Si-Si}
1843.6	3.3	1843.8	3.1	1843.7	3.2	1842.6	3.1	σ^*_{Si-C}
						1844.2	1.5	σ^*_{Si-C}
1844.6	2.3	1844.5	2.4	1844.5	2.4			σ^*_{Si-O}, σ^*_{Si-C}
1846.9[b]		1846.9[b]		1846.9[b]		1845.7[b]		IP
1849	−2.1	1848.6	−1.7	1847.7	−0.8	1849	−3.3	σ^*_{Si-C}
1856	−9	1856	−9	1856	−9	1855	−9	EXAFS

[a] Monochromator energy scale was set by previous recording of the Si 1s spectrum of crystalline Si (edge inflection set at 1839.2 eV).[14,24] [b] Si 1s IPs were estimated from the Si 2p IPs by assuming the Si 2p−Si 1s splitting is the same as the Si Kα X-ray energy (1740 eV).[49] IP of Me_3SiOH estimated from the IP of Me_3SiOMe.

mixing of Si atomic orbitals (AOs) and the π^* orbitals of the phenyl ring. The absence of a feature at this energy in the Si 1s spectra of the corresponding Me_3Si-X species is support for our attribution of the ∼1842 eV peak in the Ph_3Si-X species to Si 1s excitation to a π^*_{Si-Ph} level. Our detailed rationalization for this assignment is postponed to the following section. First, we will discuss the other Si 1s spectral features.

As expected from previous work on $Me_3SiSiMe_3$,[16,17] $Ph_3SiSiPh_3$ also exhibits a low-energy peak at 1842.7 eV. There is no counterpart in the spectra of any of the nondisilane species. This feature is attributed to S 1s → σ^*_{Si-Si} excitations, where σ^*_{Si-Si} is the LUMO, which has a large Si−Si antibonding character. The somewhat higher energy of this feature in $Ph_3SiSiPh_3$ is likely a consequence of the interaction of the low-lying σ^*_{Si-Si} and π^*_{Si-Ph} levels. An analogous effect, namely strong π(phenyl) and σ(Si−Si) mixing, has been reported in the valence photoelectron spectra of phenyl-substituted disilanes.[42]

The Si 1s spectra of the two Ph_3Si-X molecules (X = OH, $OSiPh_3$), which have an identical next-neighbor chemical environment of Si, are very similar. The Si 1s spectra of Me_3SiOH, Me_3SiOMe, and $Me_3SiOSiMe_3$ are also quite similar, but different from the spectra of the corresponding Ph_3Si-X species. The similarity of the pair (Ph_3Si-OH, $Ph_3Si-O-SiPh_3$) and the triplet (Me_3SiOH, $Me_3SiOSiMe_3$, Me_3SiOMe) indicates that Si 1s excitation is not greatly affected by the nature of the Y group in these $Me_3Si-O-Y$/$Ph_3Si-O-Y$ species. We were somewhat surprised by this observation because the Si−O bond strength differs by 10% among the molecules $Me_3Si-O-Y$, Y = H, Me, $SiMe_3$.[3] If this bond strength difference was caused by differences in a covalent bonding interaction, such as hyperconjugation, then we would expect to see changes in excitations involving σ^*_{Si-O} levels. However if Si−O bonding is predominantly (but not entirely) ionic as some have argued,[10] then there should be very little dependence of the Si 1s spectrum on the nature of the Y group. The absence of any spectral dependence on the nature of the Y group in either the $Me_3Si-O-Y$ or $Ph_3Si-O-Y$ series supports interpretations which stress large ionic contributions to the Si−O−Y bond.

At somewhat higher energy (∼1845 eV), a strong, broad peak is seen in the two $Ph_3Si-O-Y$ species. A similar but less symmetric feature is seen in the corresponding $Me_3Si-O-Y$ species. We attribute these peaks to an overlap of excitations to orbitals of σ^*_{Si-O} and σ^*_{Si-C} character, with $2\pi^*_{Si-Ph}$ contribution in the Ph_3Si-X species (see section 3.2). In the hexaphenyldisilane species, the ∼1845 eV feature is relatively weak, since it lacks the σ^*_{Si-O} contribution. At higher energy (>1850 eV), the Si 1s continua of all three Ph_3Si-X compounds are relatively similar, each exhibiting a two peak pattern which is remarkably similar to that found in the C 1s spectrum of benzene (at 294 and 300 eV in Figure 4). The Si 1s continua for the Me_3Si-X species are distinctly different. These observations suggest interpretation of the 1850 and 1862 eV peaks in the Ph_3Si-X species as Si 1s → $1\sigma^*_{C=C}$ and Si 1s → $2\sigma^*_{C=C}$ transitions, respectively. This is a rather surprising suggestion since one normally would expect poor spatial overlap. However, previous studies have found that delocalization often occurs simultaneously in both the π^* and σ^* manifolds.[32] Thus, the π^*_{Si-Ph} features at ∼1842 and 1844.5 eV and these two continuum features ascribed to $\sigma^*_{C=C}$ provide a consistent picture of extensive delocalization from the phenyl ring to the Si atom, which does not occur in the corresponding Me_3Si species. Note that this picture of extensive delocalization and mixing of Si and phenyl ring orbitals (both π^* and σ^*) is further supported by the Si 2p spectra (see section 3.3).

3.2. π Delocalization across the Si−C_{Phenyl} Bond. Figure 2 compares the experimental Si 1s spectrum of

(42) Pitt, C. G.; Bock, H. *J. Chem. Soc., Chem. Commun.* **1972**, 28.

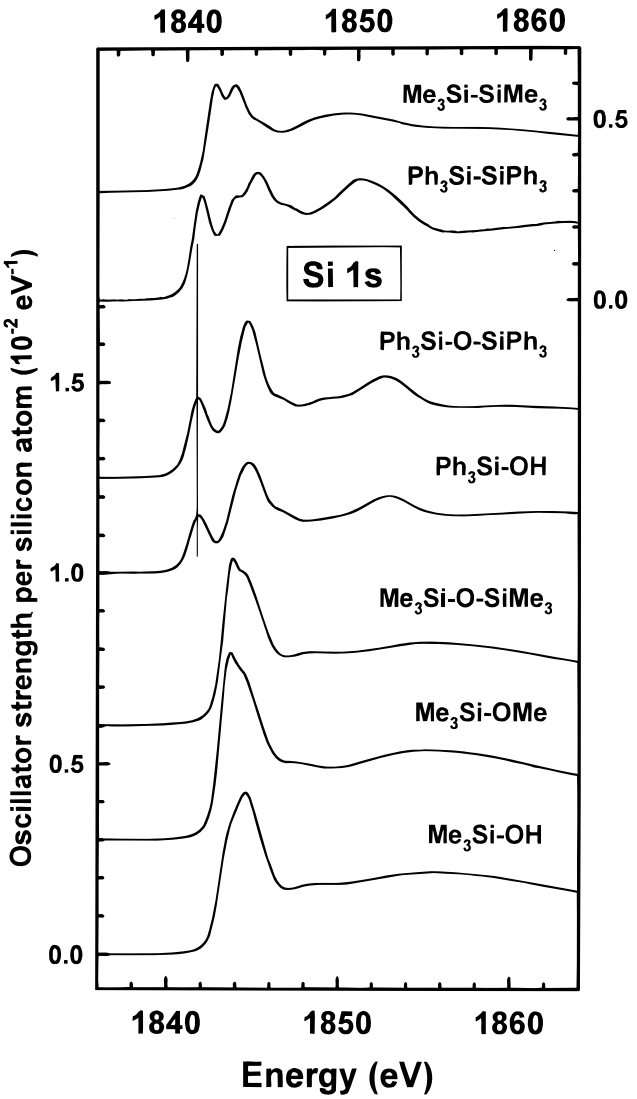

Figure 1. Oscillator strength spectra in the region of Si 1s excitation of hexaphenyldisilane (s), hexamethyldisilane (g), hexaphenyldisiloxane (s), triphenylsilanol (s), hexamethyldisiloxane (g), trimethylmethoxysilane (g), and trimethylsilanol (g). The solid state spectra were recorded with sample current detection, while the gas phase spectra were recorded using total ionization yield detection. The energy scales of the two disilane spectra (top scale) are shifted by 1.3 eV relative to the energy scales of the five triphenyl and trimethyl Si−O species (bottom scale) to account for the ionization potential difference between the disilane (Si−Si) and Si−O bonded species.

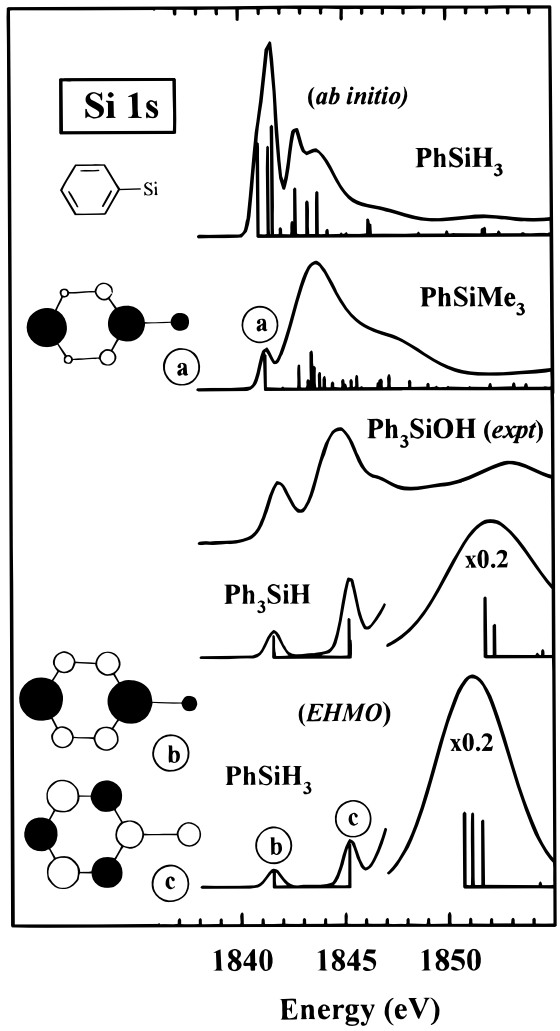

Figure 2. Comparison of the experimental Si 1s spectrum of Ph_3SiOH to the spectra of $PhSiH_3$ and Ph_3SiH, predicted by EHMO calculations carried out using the EICVOM ($Z + 1$) approach, and the spectra of $PhSiH_3$ and $PhSiMe_3$, predicted by *ab initio* calculations. See text for further details of the calculation and spectral generation. The MO sketches indicate the np_z contributions to selected low energy unoccupied molecular orbitals of core excited $PhSiMe_3$: (a) calculated by *ab initio* methods and $PhSiH_3$ (b,c) calculated by EHMO methods. The area of each circle is proportional to the C 2p−π or Si3p−π density. For the EHMO MOs, the orbital contribution on silicon is multiplied by three for better visualization.

Ph_3SiOH to the EHMO-predicted Si 1s spectra of $PhSiH_3$ and Ph_3SiH and the *ab-initio*-predicted Si 1s spectra of $PhSiH_3$ and $PhSiMe_3$. The high-energy portion of the EHMO-calculated spectra are reduced in intensity by a factor of five in order to compensate for an artificially strong σ^*_{Si-H} contribution. The molecule $PhSiH_3$ was chosen as a simple model for examining Si 1s excitation in phenylsilanes. The EHMO spectrum of $PhSiH_3$ predicts two weak, low-energy Si 1s → π^* transitions. Sketches of the π-contribution to the molecular orbitals associated with the two low-lying features in $PhSiH_3$ (b,c) are used to examine the character of the core excited states. The area of each circle is proportional to the π-orbital density on the atom. Peak b corresponds to Si 1s excitation into the lowest unoccupied MO (LUMO) in $PhSiH_3$, an orbital in which the LUMO phenyl $1\pi^*$ level (e_{2u} in benzene) is delocalized onto Si; the second transition, peak c, involves a Si 1s state in which there is delocalization of the second lowest phenyl $2\pi^*$ level (b_{2g} in benzene) onto Si. In both cases, the orbital has π-overlap (in phase) between Si and the C−R carbon of the phenyl ring but it is clearly of π^* character on the phenyl group. We refer to such states as having π^*_{Si-Ph} character in view of the orbital character on the phenyl ring, even though this labeling is formally incorrect because there is no orbital node at the Si−Ph bond. The nature of this orbital suggests there may *not* be a corresponding occupied Si−C π-bonding molecular orbital (i.e., one involving an in-phase mix of a Si 3p orbital with a π orbital on the phenyl ring). On the basis of the position of the second peak in the EHMO spectrum, the feature at ∼1844.5 eV in the Ph_3-

SiOH spectrum likely contains contributions from the Si 1s → $2\pi^*_{C=C}$ transitions.

The large difference in intensity between the EHMO-calculated and the experimental Si 1s → π^*_{Si-Ph} transition (relative to the higher energy Si 1s → σ^* features) led us to question the validity of the EHMO calculations in this context. One might rationalize the low Si 1s → π^*_{Si-Ph} intensity in terms of the single phenyl coordination in $PhSiH_3$, relative to the triphenyl coordination of Ph_3SiOH. This possibility was examined by comparing the EHMO calculation of the Si 1s spectrum of $PhSiH_3$ to that of Ph_3SiH. While the π^* features are slightly more intense in the triphenylsilane molecule (and the higher energy σ^*_{Si-H} features are diminished), the weakness of the π^* features remains.

In order to provide further confirmation of the identity and assignment of the EHMO π^* features, *ab initio* calculations were performed for $PhSiH_3$. These are also presented in Figure 2. Unlike the EHMO spectrum of $PhSiH_3$, there is no clearly separated π^* transition(s) at low energy, but rather many closely spaced transitions. Examination of the MO character of the calculated core excited states shows that the lowest feature is in fact the Si 1s → $1\pi^*$ transition and the next two intense features are of mixed σ^*_{Si-H}−Rydberg character. The presence of low-lying Si 1s → σ^*_{Si-H}−Rydberg transitions in $PhSiH_3$ is consistent with literature assignments of the Si 1s spectrum of silane.[43] In order to remove the "interference" associated with the Si−H bonds, we wanted to compare our experimental results with an *ab initio* calculation of the triphenyl species (Ph_3SiH; $C_{18}H_{16}Si$). However, this is presently beyond our computational resources at this level of theory. Instead, we have carried out an *ab initio* calculation for Si 1s excitation of $PhSiMe_3$. Replacement of the hydrogen atoms with methyl groups eliminates the strong Si 1s → σ^*_{Si-H}−Rydberg transitions. While $PhSiMe_3$ is substantially different from Ph_3SiOH, it allows visualization of the low-lying Si 1s → π^* feature(s) without interference from the (accurate) prediction of the Si 1s → σ^*_{Si-H} transitions. The calculated spectrum of $PhSiMe_3$ has a single low-energy feature at approximately the same energy as the feature we assign as Si 1s → π^*_{Si-Ph} in Ph_3SiOH. As shown in Figure 2 (sketch a), the π-$2p_z$ contribution to the lowest MO of $PhSiMe_3$ calculated by GSCF3 is very similar to that of the lowest π^* in the EHMO calculation of $PhSiH_3$. Detailed examination of the higher lying MOs reveals the Si 1s → π^* transition at ∼1843 eV hiding in a forest of Si 1s → σ^*_{Si-C} transitions.

At first glance, the existence of a LUMO of π^*_{Si-Ph} character in Ph_3Si-X species is unusual because silicon is tetrahedrally coordinated in these species and, thus, one does not expect any formal Si−Ph π bonding. Si core → π^* features have been observed for several undercoordinated silicon species, including silylenes[18] with cyclic π delocalization, and SiO,[44] which has a formal Si=X π bond. The observation of π interactions with tetrahedral silicon is not necessarily surprising, as other experiments have shown phenomena which can be explained in a similar manner. For example, in *tert*-butyl- and trimethylsilyl-substituted polyacetylenes ($Me_3X-(CC)_n-XMe_3$, X = C, Si), a stabilization in the HOMO binding energy (acetylene π) is seen when carbon is replaced by silicon. This largely arises from the inductive effect of the silicon group.[45] However, the $\pi \rightarrow \pi^*$ transition of these systems shows a *decrease* in transition energy when carbon (*tert*-butyl) is replaced by silicon (trimethylsilyl).[45] This suggests that there must be a strong Si−phenyl π^* interaction that lowers the energy of the LUMO π^* level. However, π and π^*

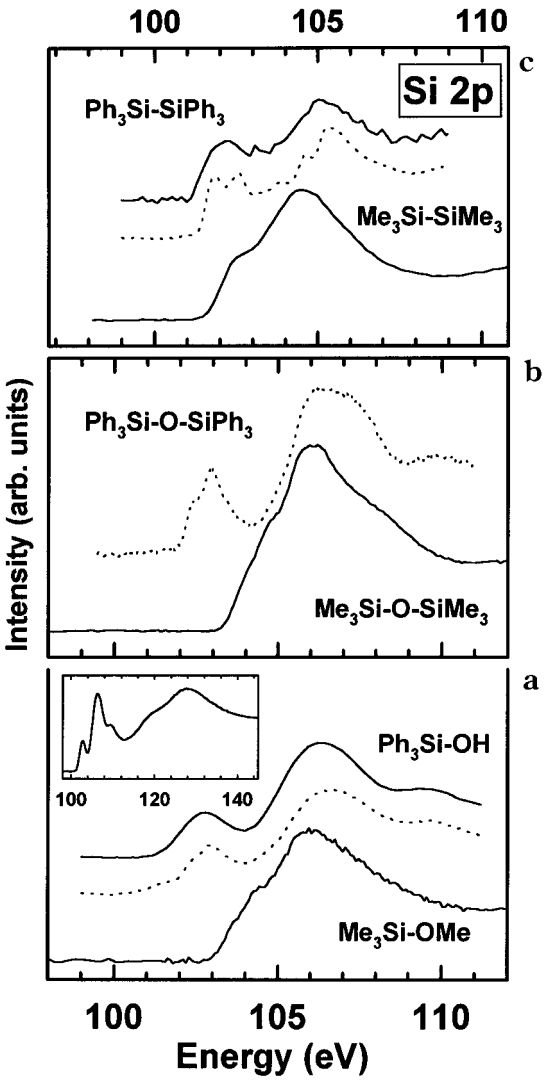

Figure 3. Si 2p gas phase energy loss spectra (solid line) and Si 2p solid state photoabsorption spectra (dotted line) of (a) triphenylsilanol (g,s) and trimethylmethoxysilane (g) (b) hexaphenyldisiloxane (s) and hexamethyldisiloxane (g) and (c) hexamethyldisilane (g) and hexaphenyldisilane (g,s). The energy scale of the upper panel (RSi−SiR) is shifted +1.2 eV relative to that of the lower two panels to take into account IP differences. A background generated by extrapolation of the pre-edge signal has been subtracted from each spectrum. The insert is the Si 2p gas phase EELS spectrum of triphenylsilanol acquired over a larger energy loss range. The energy loss spectra were recorded using a 2.5 keV final electron energy, ∼2° scattering angle, and 0.7 eV fwhm resolution. A background generated by extrapolation of the pre-edge signal has been subtracted from each spectrum.

(43) Bodeur, S.; Millié, P.; Nenner, I. *Phys. Rev. A* **1990**, *41*, 252.
(44) Flank, A. M.; Karnatak, R. C.; Blancard, C.; Esteva, J. M.; Lagarde, P.; Connerade, J. P. *Z. Phys. D* **1991**, *21*, 357. Bouisset, E.; Esteva, J. M.; Karnatak, R. C.; Connerade, J. P.; Flank, A. M.; Lagarde, P. *J. Phys. B: At., Mol. Opt. Phys.* **1991**, *24*, 1609.

(45) Bock, H.; Seidl, H. *J. Chem. Soc. B* **1968**, 1158. Eastmond, R.; Johnson, T. R.; Walton, D. R. M. *Tetrahedron* **1972**, *28*, 4601.

Table 2. Energies, Term Values, and Proposed Assignments for Features in the Si 2p Photoabsorption Spectra of (A) Triphenylsilanol, Hexaphenyldisiloxane, and Hexaphenyldisilane and (B) Trimethylmethoxysilane, Hexamethyldisiloxane, and Hexamethyldisilane

(A) Ph_3Si-X (Gas, EELS; Solid, Total Electron Yield Photoabsorption)

Ph_3Si-OH				$Ph_3Si-O-SiPh_3$			$Ph_3Si-SiPh_3$					
E (eV)		solid		*E* (eV)	solid		*E* (eV)		solid		assignments	
gas	solid	$T_{3/2}$	$T_{1/2}$	solid	$T_{3/2}$	$T_{1/2}$	gas	solid	$T_{3/2}$	$T_{1/2}$	3/2	1/2
102.8[a]	102.3	4.3		102.4	4.2		102.2	101.7	3.7		π^*_{Si-Ph}	
	102.9		4.3	102.9		4.3		102.5		3.5		π^*_{Si-Ph}
								103.9	1.5		σ^*_{Si-Si}	
							104.3 (sh)	104.6	0.8		σ^*_{Si-C}	
							105.2	105.3		0.7		σ^*_{Si-C}
106.3	106.7(3)	0.2[b]		106.3	0.6[b]							σ^*_{Si-O}
106.6[c]				106.6[c]			105.4[c]				IP ($2p_{3/2}$)	
107.2[c]				107.2[c]			106.0[c]					IP ($2p_{1/2}$)
109.5	109.7	−2.8[b]		109.8	−2.9[b]						σ^*_{Si-C}	
120		−13									Si 2p → ϵd	
127.6		−21									Si 2p → ϵd	

(B) $MeSi-X$ (Gas, EELS)

$Me_3Si-OMe$		$Me_3Si-O-SiMe_3$		$Me_3Si-SiMe_3$		
E (eV)	T^b	*E* (eV)	T^b	*E* (eV)	T^b	assignment
				102.6	3.1	σ^*_{Si-Si}
104.3	2.6	104.4	2.5	104.5	1.2	σ^*_{Si-C}
106.0[a]	0.9	105.9[a]	1.0			σ^*_{Si-O}
106.6[d]		106.6[d]		105.4[d]		IP($2p_{3/2}$)
107.2[d]		107.2[d]		106.0[d]		IP($2p_{1/2}$)
108	−1.1	108	−1.1			σ^*_{Si-C}, EXAFS
114	−7.1	114	−7.1	112	−6	Si 2p → ϵd
128	−21	128	−21	125	−19	Si 2p → ϵd

[a] Calibration: triphenylsilanol, −81.7 eV relative to (S $2p^{-1}$,t_{2g}) of SF_6; hexaphenyldisilane, as for photoabsorption spectrum; trimethylmethoxysilane, −78.5(1) eV relative to SF_6; hexamethyldisiloxane, −184.9(2) relative to π^* of CO_2; hexamethyldisilane, −186.28(8) relative to CO_2. [b] Where only a single term value is listed, this refers to the average Si 2p IP. [c] Vertical Si $2p_{3/2}$ IPs for Ph_3SiX species estimated from XPS measurements for Me_3SiOMe,[50] $Me_3SiOSiMe_3$,[51] and $Me_3SiSiMe_3$[50,51] (Me = methyl). Si $2p_{1/2}$ IPs are 0.61 eV higher.[50,52] [d] XPS.[50,51]

interactions are not expected in nonplanar molecules, and thus, it is appropriate to characterize these effects when they are observed. Core excitation spectroscopy is clearly useful in this context.

3.3. Si 2p Spectra. The Si 2p electron energy loss spectra (solid lines) of gas phase $Ph_3SiSiPh_3$, $Me_3SiSiMe_3$, $Me_3SiOSiMe_3$, Ph_3SiOH, and Me_3SiOMe are presented in Figure 3, in comparison to the Si 2p TEY photoabsorption spectra (dotted lines) of $Ph_3SiSiPh_3$, $Ph_3SiOSiPh_3$, and Ph_3Si-OH. The Si 2p spectrum of $Me_3SiSiMe_3$, recorded at medium resolution by ISEELS and high-resolution photoabsorption, has been reported and analyzed in detail elsewhere.[16,17] Energies, term values, and proposed assignments are presented in Table 2. The Si 2p spectrum of Me_3SiOMe is in good agreement with those reported earlier by Winkler et al.,[46] using ISEELS, and by Sutherland et al.,[15] using X-ray photoabsorption.

In the spectra of all three Ph_3Si-X species, there is a strong low-energy feature peaking around 102−103 eV, which is absent in the spectra of the three Me_3Si-X species. The same features are observed in the higher energy resolution photoabsorption spectra of the three Ph_3Si-X molecules, but with the characteristic 0.6 eV Si 2p spin−orbit splitting detected. We attribute the 102−103 eV peak in the Ph_3Si-X species to core → valence-type transitions where the upper orbital of the transition has significant π^*_{Si-Ph} character.

The spectra of the four molecules containing Si−O bonds exhibit an intense broad feature peaking around 106 eV. These are attributed to Si 2p → σ^*_{Si-O} excitations. At somewhat lower energy (∼105 eV), there is a broad shoulder which we attribute to Si 2p → σ^*_{Si-C} transitions. We might expect a Si 2p → $2\pi^*_{Si-Ph}$ transition above the Si 2p → σ^*_{Si-O} transitions in the Ph_3Si-X species, in analogy to that observed in the Si 1s spectra. While a discrete transition is not resolved, the Si 2p → σ^*_{Si-O} transition in the Ph_3Si-X species is broader and is shifted to higher energy than the similar feature in the Me_3Si-X species. It is possible that the additional broadening is associated with a Si 2p → $2\pi^*_{Si-Ph}$ contribution.

In $Ph_3SiSiPh_3$, we expect to observe a Si 2p → σ^*_{Si-Si} transition, by analogy to its Si 1s spectrum and the observation of a Si 2p → σ^*_{Si-Si} transition in $Me_3SiSiMe_3$.[16,17] This transition is not resolved, but it is likely that it "fills in" the space between the π^*_{Si-Ph} feature (102 eV) and the σ^*_{Si-C} structure at 105 eV. Recently Gardelis et al.[54] have used S 2p spectral features at 102 and 106 eV, assigned to σ^*_{Si-Si} and σ^*_{Si-O} resonances, to characterize relative amounts of Si−Si and Si−O bonds in porous silicon samples.

The Si 2p spectra of all species exhibit further structure at higher energies (see the extended range energy loss spectrum of gas phase Ph_3SiOH in the insert to Figure 3). In addition to the features discussed above, there are a number of broad features, such as those occurring at 109.5, 120, and 127.6 eV in Ph_3SiOH. These higher energy features are attributed to a combination of higher order σ^* excitations and to the intrinsic shape of the Si 2p ionization continuum,[15,46] which is characterized by a delayed onset of 2p core

(46) Winkler, D. C.; Moore, J. H.; Tossell, J. A. *Chem.Phys. Lett.* **1994**, *222*, 1.

Table 3. Energies, Term Values, and Proposed Assignments for Features in the C 1s EELS Spectra of (A) Benzene, Triphenylsilanol, and Hexaphenyldisilane and (B) Trimethylmethoxylsilane, Hexamethydisiloxane, and Hexamethyldisilane

(A) Ph_3Si-X

C_6H_6[a]		Ph_3Si-OH		$Ph_3Si-SiPh_3$		
E (eV)	*T*	*E* (eV)	*T*	*E* (eV)	*T*	assignment[c]
285.3	5.0	285.1[d]	5.2	285.1[d]	5.2	$1\pi^*(e_{2u})$
287.2	3.1	287.6	2.7	287.3	3.0	3p
288.9	1.4	289.0	1.3	288.8	1.5	$2\pi^*(b_{2g})$
290.3[b]		290.3[e]		290.3[e]		IP
293.5	−3.2	293.4	−3.1	293.4	−3.1	$1\sigma^*(e_{1u})$
300	−10	301	−11			$2\sigma^*(e_{2g} + a_{2g})$

(B) Me_3Si-X

$Me_3Si-OMe$		$Me_3Si-O-SiMe_3$		$Me_3Si-SiMe_3$[f]		
E (eV)	*T*	*E* (eV)	*T*	*E* (eV)	*T*	assignment[c]
286.3	3.5	286.0	3.7	286 (sh)	3.7	3s
287.3[d]	2.5	287.3[d]	2.4	287.4[d]	2.3	3p/C−H
290.2	−0.4					σ^*_{C-O}, σ^*_{C-Si}
		289.6	0.1	290	−0.3	σ^*_{C-Si}
289.8[e]		289.7[e]		289.7[e]		IP

[a] From ref 47. [b] From gas phase XPS, relative to vacuum level.[53] [c] Only the final orbital is listed. [d] Calibration relative to C 1s → π^* in CO_2 (290.74 eV):[20,21] Ph_3Si-OH $E = -5.69(1)$ eV; $Ph_3Si-SiPh_3$ $E = -5.67(6)$; $Me_3Si-OMe$ $E = -3.39(4)$ eV; $Me_3Si-O-SiMe_3$ $E = -3.40(4)$ eV; $Me_3Si-SiMe_3$ $E = -3.43(5)$ eV. [e] IPs for Ph_3SiX species are estimated from C 1s IP of C_6H_6 (290.3 eV):[53] IPs for $Me_3SiSiMe_3$ and Me_3SiOMe estimated from C 1s IP of $Si(Me)_4$ (289.78 eV) and of $Me_3SiOSiMe_3$ (289.72 eV).[51] [f] Also reported in ref 16.

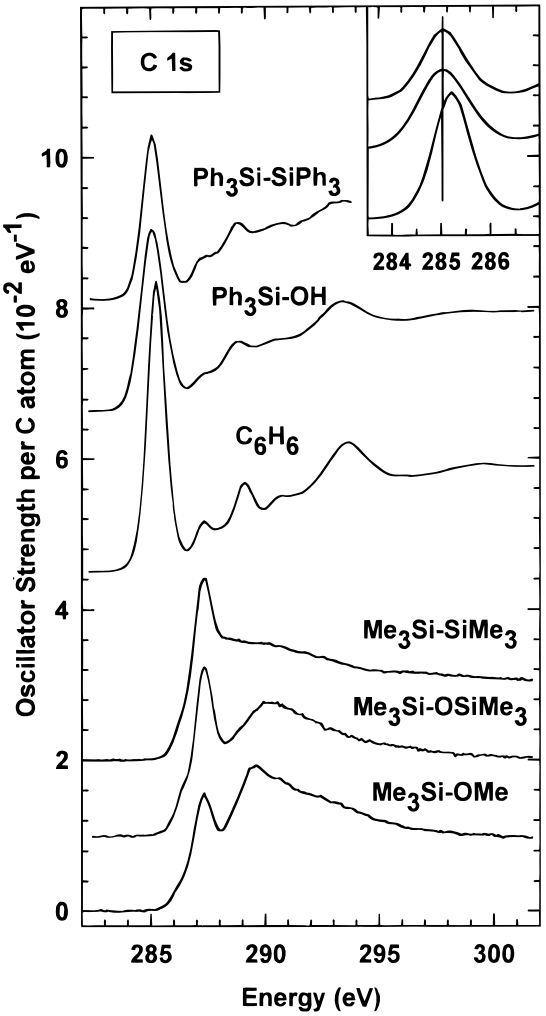

Figure 4. C 1s oscillator strength spectra of benzene,[47] triphenylsilanol, hexaphenyldisilane, trimethylmethoxysilane, hexamethyldisiloxane, and hexamethyldisilane[16] derived from dipole-regime EELS (see caption to Figure 3 for experimental details). The insert is an expanded presentation of the phenyl π^* peak illustrating the changes in position and line shape between benzene and the phenylsilanes.

ionization caused by the angular momentum barrier in the dominant 2p → ϵd channel.

3.4. C 1s Spectra. Figure 4 compares the C 1s oscillator strength spectra derived from inner shell electron energy loss spectra of Ph_3SiOH, $Ph_3SiSiPh_3$, benzene,[47] Me_3SiOMe, $Me_3SiOSiMe_3$, and $Me_3SiSiMe_3$.[16] The energies, term values, and proposed assignments of the spectral features are presented in Table 3, along with the results for benzene from the literature.[47] Not surprisingly, the C 1s spectra of both phenylsilane species are essentially benzene-like, since the environment of most of the C atoms is approximately the same in all three molecules. The Si−Si bond in $Ph_3SiSiPh_3$ does not introduce any additional low-lying feature in the C 1s spectrum, in contrast to the situation in the Si core spectrum, suggesting that C 1s → LUMO (σ^*_{Si-Si}) excitation in this compound has negligible intensity. At first sight, the overall similarity of the C 1s spectra of the Ph_3SiX species to that of benzene appears inconsistent with our interpretation of the Si core level spectra as involving low-lying excitations to π^*_{Si-Ph} orbitals, since one might expect corresponding excitations in the C 1s spectra. However, the C−Si signal should only be $^1/_6$ of the total C 1s signal, and thus, it will be overshadowed by that of the C−H carbons. There is little difference in electronegativity between the C−H and C−Si carbons, so there should not be any significant chemical shift of the C 1s energy. The greater breadth of the $\pi^*_{C=C}$ (285 eV) transition and the shift of the centroid by 0.2 eV to lower energy may be the signature of π^*_{Si-Ph} contributions and delocalization across the Si−phenyl bond (see the insert to Figure 4). Higher energy resolution spectra would be of great interest as the $1\pi^*_{C=C}$ and π^*_{Si-Ph} features might be resolved.

The dominant lowest energy feature in the C 1s spectrum of each Ph_3SiX species corresponds to excitations to π^* orbitals, which correlate with the $1\pi^*(e_{2u})$ orbital of benzene. The peaks at 287−288 eV are attributed to C 1s → Rydberg transitions. The feature

(47) Horsley, J. A.; Stöhr, J.; Hitchcock, A. P.; Newbury, D. C.; Johnson, A. L.; Sette, F. *J. Chem. Phys.* **1985**, *83*, 6099.

around 289 eV is assigned to one-electron C 1s → π^*-(b_{2g}) transitions. Experimental and theoretical studies of benzene suggest this state is one in which the one-electron (C $1s^{-1}$, $\pi^*(b_{2g})$) configuration is heavily mixed with the (C $1s^{-1}$, π^{*-1}, π^{*2}) multielectron excited configuration.[48] Interestingly, the $2\pi^*$ (b_{2g} in benzene) feature for Ph_3Si-X is less prominent and apparently less intense than that for benzene. This may be a further manifestation of the Si−Ph delocalization. At higher energy, the C 1s continuum of Ph_3Si-OH exhibits a two peaked pattern very similar to that of benzene[47] and, thus, these features are attributed to C 1s → $\sigma^*_{C=C}$ transitions.

The C 1s spectra of Me_3SiOMe, $Me_3SiOSiMe_3$, and $Me_3SiSiMe_3$ (Figure 4) are rather similar to the C 1s spectra of saturated hydrocarbons, such as ethane. The relatively sharp peak at 287 eV is attributed to excitation to a level of mixed valence−Rydberg character with σ^*_{C-H} valence and 3p Rydberg character. The shoulder around 286 eV is the 3s Rydberg level. The broad peak at 289.5−290 eV is mainly σ^*_{C-Si} in character. This C 1s → σ^*_{C-Si} feature is substantially stronger in $Me_3SiOSiMe_3$ than in $Me_3SiSiMe_3$, even though the next-neighbor environment of carbon is identical in both molecules. In Me_3SiOMe, this feature is stronger because it also contains the C 1s (MeO) → σ^*_{C-O} resonance.

4. Summary

Core excitation spectra at the Si 1s, Si 2p, and C 1s edges were recorded for a range of triphenylsilyl and trimethylsilyl species in the gas and/or solid state. There is excellent agreement between the gas and solid state spectra for the same edge of the same molecule, suggesting the spectra are dominated by valence-type excitations and that electronic interactions in the solid make little change to the molecular electronic structure in the region of the molecule sampled by core excitation. Assignments for all spectral features have been proposed. The Si 1s spectrum of each Ph_3Si-X species exhibits a low-lying feature (~1842 eV), which we interpret as Si 1s → $1\pi^*_{Si-Ph}$ transitions. This assignment is consistent with the absence of a π^* feature in the Si 1s spectra of all Me_3Si-X species and is supported by EHMO and *ab initio* calculations, both of which predict delocalization of phenyl π^* orbital density onto Si in Ph_3Si-X species. We note that both the low-level semi-empirical EHMO ($Z + 1$) calculation and the high-level *ab initio* calculation played important roles in developing our interpretation of these spectra. Calculations of large molecules are trivial with extended Hückel, but occasionally the results are not entirely convincing. While high-level *ab initio* calculations are limited to smaller molecules, their results are often more accurate. Simplified model systems can thus be examined by *ab initio* methods, but one must be careful that spectral features associated with inappropriate aspects of a simplified molecular model do not complicate the spectral interpretation, as was the case in the *ab initio* calculation for $PhSiH_3$.

Low-lying σ^*_{Si-Si} states are observed in the Si 1s and Si 2p spectra of $Ph_3Si-SiPh_3$ and $Me_3Si-SiMe_3$, further supporting the generality of a previously formulated hypothesis that molecules containing Si−Si bonds exhibit low-lying core excited states associated with excitations to an orbital with large σ^*_{Si-Si} character.[16,17] Comparison of the Si 1s spectra of $Ph_3Si-SiPh_3$ and $Me_3Si-SiMe_3$ indicates that the σ^*_{Si-Si} state in $Ph_3Si-SiPh_3$ is perturbed by interaction with the phenyl levels. Finally, silicon core excitation spectra are relatively unaffected by the nature of the Y group in $Ph_3Si-O-Y$ or $Me_3Si-O-Y$ compounds, indicating that the nature of the Y substituent does not affect the unoccupied electronic structure at Si. This result, which is rather surprising given the well-known dependence of Si−O bond strength on the nature of Y, may reflect an appreciable ionic character of the Si−O bond.

Acknowledgment. This work is based upon research conducted at the Chemistry Department, McMaster University and at the Synchrotron Radiation Center, University of Wisconsin—Madison. Mass spectra were recorded at the McMaster Regional Centre for Mass Spectrometry. We thank the staff of the SRC for their expert operation of Aladdin, which is supported by the NSF under award no. DMR-9212658. We also thank Professor West for the use of his laboratory in Madison for the Me_3SiOH synthesis. This work has been supported financially by NSERC (Canada). C.C.T. acknowledges CNPq (Brasil) for support of a fellowship, while S.G.U. acknowledges the support of an Ontario Graduate Fellowship.

OM961028F

(48) Schwarz, W. H. E.; Chang, T. C.; Seeger, U.; Hwang, K. H. *Chem. Phys.* **1987**, *117*, 73. Bader, M.; Haase, J.; Frank, K.-H.; Ocal, C.; Puschmann, A. *J. Phys. (Paris)* **1986**, *47*, C8−501. Ågren, H.; Vahtras, O.; Carravetta, V. *Chem. Phys.* **1995**, *196*, 47.

(49) Li, D.; Bancroft, G. M.; Kasrai, M.; Fleet, M. E.; Feng, X. H.; Tan, K. H.; Yang, B. X. *Solid State Commun.* **1993**, *87*, 613.

(50) Sutherland, D. G. J.; Bancroft, G. M.; Tan, K. H. *J. Chem. Phys.* **1992**, *97*, 7918.

(51) Jolly, W. L.; Bomben, K. D.; Eyermann, C. J. *At. Data Nucl. Data Tables* **1984**, *31*, 109.

(52) Kelfve, P.; Blomster, B.; Siegbahn, H.; Siegbahn, K.; Sanhueza, E.; Goscinski, O. *Phys. Scr.* **1980**, *21*, 75.

(53) Davis, D. W.; Shirley, D. A. *J. Electron Spectrosc. Relat. Phenom.* **1974**, *3*, 157.

(54) Gardelis, S.; Bangert, U.; Hamilton, B.; Pettifer, R. F.; Hill, D. A.; Keyse, R.; Teehan, D. *Appl. Surf. Sci.* **1996**, *102*, 408.